

Electroweak Bubbles and Sphalerons

Yves Brihaye

Faculté des Sciences, Université de Mons-Hainaut B-7000 Mons Belgium

Jutta Kunz

Instituut voor Theoretische Fysica, Rijksuniversiteit Utrecht, The Netherlands

and

FB Physik, Postfach 2503, Universität Oldenburg, Germany

Abstract

We consider non-perturbative solutions of the Weinberg-Salam model at finite temperature. We employ an effective temperature-dependent potential yielding a first order phase transition. In the region of the phase transition, there exist two kinds of static, spherically symmetric solutions: sphalerons and bubbles. We analyze these solutions as functions of temperature. We consider the most general spherically symmetric fluctuations about the two solutions and construct the discrete modes in the region of the phase transition. Sphalerons and bubbles both possess a single unstable mode. We present simple approximation formulae for these levels.

Mons-Preprint

Utrecht-Preprint THU-93/09

April 1993

1) Introduction

The Weinberg-Salam model describes the electroweak interactions in the perturbative regime with remarkable accuracy. The model also predicts non-perturbative processes, such as instanton or sphaleron induced transitions, leading to baryon number violation. The suggestion [1] that the baryon asymmetry of the universe may possibly be explained within the standard model or its variants, recently created much interest in electroweak sphalerons and bubbles, non-perturbative solutions of the model.

Sphalerons [2] are relevant for baryon number violating processes in the early universe [3-5]. At a given temperature the rate of baryon number violation is largely determined by the three-dimensional action of the sphaleron solution, which enters in the Boltzmann factor, while the preexponential factor contains the frequencies of small oscillations about the sphaleron [3]. If the rate is large enough, the baryon asymmetry of the universe may be generated during the electroweak phase transition.

However, for the creation of the baryon asymmetry of the universe during a first order electroweak phase transition, the details of this phase transition turn out to be important and need to be better understood [6-11]. The first order phase transition proceeds via the creation of bubbles of the new broken phase embedded in the surrounding unbroken phase. The rate for the creation of bubbles is largely determined by the three-dimensional action of the bubble solution, which enters in the Boltzmann factor, while the preexponential factor contains the frequencies of small oscillations about the bubble [7].

Bubbles and sphalerons both arise as non-perturbative solutions of the finite temperature electroweak field theory. In the effective potential approach [12], the “Mexican hat” Higgs potential of the electroweak model is supplemented by temperature dependent terms. It is the presence of a term cubic in the Higgs field which renders the phase transition first order.

The sphaleron of the electroweak theory, present at zero temperature, persists at finite temperature up to the region of the phase transition [13]. In contrast, the bubble solution exists only at finite temperature, in the region of the phase transition [7]. Here we study these non-perturbative solutions of the temperature dependent model in the region of the phase transition. In the first part of the paper we discuss the properties of these solutions, e. g. we address their three-dimensional action, their shape and their size. In the second part of the paper we analyze the discrete modes about these

solutions. We consider the most general spherically symmetric fluctuations, diagonalize the quadratic form in these fluctuations and compute the eigenvalues of the normal modes. We find that both sphalerons and bubbles possess a single unstable mode. For the negative eigenvalues we present approximation formulae. We relate the discrete modes of the bubble to those of the antikink.

2) Lagrangian and effective potential

We consider the electroweak theory in the limit of zero mixing angle. The bosonic part of the Lagrangian reads

$$\mathcal{L} = -\frac{1}{4}F_{\mu\nu}^a F^{a\mu\nu} + (D_\mu\Phi)^\dagger(D^\mu\Phi) - V(\phi, T) , \quad (1)$$

$$\phi(x) = \sqrt{2}(\Phi^\dagger\Phi)^{\frac{1}{2}} ,$$

with the covariant derivative and field strength tensor

$$D_\mu\Phi = (\partial_\mu - i\frac{g}{2}\tau^a A_\mu^a)\Phi , \quad (2)$$

$$F_{\mu\nu}^a = \partial_\mu A_\nu^a - \partial_\nu A_\mu^a + g\epsilon_{abc}A_\mu^b A_\nu^c . \quad (3)$$

$V(\phi, T)$ denotes the temperature dependent effective potential [4,9-11]

$$V(\phi, T) = \frac{\lambda}{4}\phi^4 - \frac{\lambda}{2}v^2\phi^2 + \frac{\gamma}{2}T^2\phi^2 - \delta T\phi^3 + c , \quad (4)$$

$$\gamma = \frac{2M_W^2 + M_Z^2 + 2M_t^2}{4v^2} , \quad (5)$$

$$\delta = \frac{2M_W^3 + M_Z^3}{4\pi v^3} , \quad (6)$$

v is the Higgs field expectation value at zero temperature, and M_W , M_Z , M_t denote the masses of the W^\pm bosons, the Z^0 boson and the top quark, and c is an adjustable constant.

The effective potential (4) gives rise to a first order phase transition, characterized by three critical temperatures. For low values of the temperature T , the minimum of $V(\phi, T)$ is attained at some value $\langle\phi(T)\rangle \neq 0$, while $\phi = 0$ corresponds to a local maximum of $V(\phi, T)$. At $T = T_c$ with

$$T_c^2 = \frac{\lambda v^2}{\gamma} \quad (7)$$

the second derivative of the potential at the origin changes sign. For $T > T_c$ the extremum $\phi = 0$ turns into a local minimum separated from the absolute minimum $\langle \phi(T) \rangle$ by a small energy barrier. The two minima become degenerate at $T = T_b$ with

$$T_b^2 = \frac{T_c^2}{1 - \frac{2\delta^2}{\lambda\gamma}} . \quad (8)$$

For $T > T_b$ the extremum $\phi = 0$ constitutes the absolute minimum of the potential. Finally at $T = T_a$ the local minimum disappears.

To study temperature dependent quantities in the region of the phase transition it is convenient to represent the temperature via the variable ξ [10]

$$\xi = \frac{\lambda\gamma}{\delta^2} \left(1 - \left(\frac{T_c}{T} \right)^2 \right) . \quad (9)$$

T_c , T_b , and T_a then correspond to $\xi = 0$, $\xi = 2$, and $\xi = \frac{9}{4}$, respectively.

Throughout the paper we employ for the masses the values $M_W = 80$ GeV, $M_Z = 92$ GeV, $M_t = 120$ GeV and $M_H = 45$ GeV, and the vacuum expectation value for the Higgs field $\langle \phi(0) \rangle = v = 246$ GeV, leading to the critical temperatures

$$T_c = 0.284v , \quad T_b = 0.292v , \quad T_a = 0.293v . \quad (10)$$

3) Non-perturbative solutions

In order to construct non-perturbative solutions of the effective lagrangian (1) we choose the gauge $A_0^a = 0$ and we employ for the fields the static, spherically symmetric ansatz

$$\Phi(\vec{r}) = \frac{v}{\sqrt{2}} L(r) \begin{pmatrix} 0 \\ 1 \end{pmatrix} , \quad A_i^a(\vec{r}) = \frac{G(r)}{gr^2} \epsilon_{iba} r_b , \quad (11)$$

where $L(r)$ and $G(r)$ are radial functions. The three-dimensional effective action is then given by the functional

$$S(T) = \frac{4\pi M_W}{g^2} \int dx x^2 \sigma(x) , \quad (12a)$$

with the action density

$$\sigma(x) = \frac{G^2(G-2)^2}{2x^2} + \left(\frac{dG}{dx} \right)^2 + 2x^2 \left(\frac{dL}{dx} \right)^2 + G^2 L^2 + \frac{16\lambda}{g^2} x^2 V(L, T) , \quad (12b)$$

the effective potential

$$V(L, T) = \frac{1}{4} \left(L^4 - 2L^2 + \frac{2\gamma T^2}{\lambda v^2} L^2 - \frac{4\delta T}{\lambda v} L^3 + c \right) , \quad (12c)$$

and the dimensionless variable

$$x = M_W r , \quad M_W = \frac{1}{2} g v .$$

The constant c in the effective potential has to be adjusted such that the integrand (12b) approaches zero asymptotically for the non-perturbative solution considered.

Sphalerons

The sphaleron, a well-known non-perturbative solution of the effective action (12) for $T = 0$, can be continued to finite temperatures, $0 \leq T < T_a$. The sphaleron functions satisfy the boundary conditions

$$G(0) = 2 , \quad G(\infty) = 0 , \quad (13a)$$

$$L(0) = 0 , \quad L(\infty) = \frac{\langle \phi(T) \rangle}{v} , \quad (13b)$$

where $\langle \phi(T) \rangle$ denotes the non-trivial minimum of $V(\phi, T)$. The profiles of $G(x)$ and $L(x)$ are presented in Fig. 1 for $T = T_c$ and $T = 0$. The action density (12b) of the sphaleron is presented for the temperatures $T = T_b$, $T = T_c$ and $T = 0$ in Fig. 2. Both figures indicate that the sphaleron radius increases from $r \approx 3M_W^{-1}$ at $T = 0$ to $r \approx 9M_W^{-1}$ for $T = T_b$.

In Fig. 3 we exhibit the three-dimensional action of the sphaleron as a function of ξ in the range of the phase transition. The three-dimensional action of the sphaleron follows an approximate scaling law,

$$S_{\text{sp}}(T) = S_{\text{sp}}(0) \frac{\langle \phi(T) \rangle}{\langle \phi(0) \rangle} . \quad (14)$$

For an effective potential without the cubic term this scaling law is exact. $S_{\text{sp}}(T)$ is well approximated by the scaling formula (14) [13]. The values predicted by the scaling formula exceed the exact numerical values only by a few percent, from 3% at $T = T_c$ up to 6% at $T = T_b$. For comparison the values obtained from the scaling formula (14) are also shown in Fig. 3. Since the scaling formula works so well, we have introduced a scaling factor

$$\Lambda = \frac{\langle \phi(T) \rangle}{\langle \phi(T_b) \rangle}$$

in Fig. 2 for the coordinate x and for the action density $\sigma(x)$. In the case of exact scaling, the three curves would be equal.

Bubbles

In the range of the phase transition $T_c < T < T_b$, the equations of motion obtained from the functional (12) admit another non-perturbative solution, the bubble. It is through the formation of bubbles, that the first order electroweak phase transition proceeds.

For the bubble solution, the gauge field consistently vanishes, $G(x) = 0$, and the equation for the Higgs field function $L(x)$ reads

$$\frac{d^2 L}{dx^2} + \frac{2}{x} \frac{dL}{dx} = \frac{4\lambda}{g^2} \left[L^3 - L \left(1 - \frac{\gamma T^2}{\lambda v^2} \right) - L^2 \left(\frac{3\delta T}{\lambda v} \right) \right]. \quad (15)$$

Choosing $c = 0$, a regular solution with finite three-dimensional action is obtained, where the function $L(x)$ satisfies the boundary conditions

$$\frac{\partial L}{\partial x}(0) = 0, \quad L(\infty) = 0, \quad (16)$$

to be contrasted with boundary condition (13b). Note, that Derrick's theorem, forbidding the existence of static solutions of finite energy of a scalar theory in three spatial dimensions, applies only to a positive definite potential.

The phase transition occurs in the temperature interval $1.3 < \xi < 1.8$ [10,11]. The bubble function $L(x)$ is presented in Fig. 4 for the temperatures $\xi = 1.3$, $\xi = 1.8$ and $\xi = 1.9$. Only when $\xi > 1.6$ the bubble starts to develop an interior region, where $L(x)$ is approximately constant. When $\xi = 1.8$ the size of this interior region is only about the size of the wall, and roughly $60M_W^{-1}$ wide. When $\xi = 1.9$ the interior region is only about twice the size of the wall. Increasing the temperature beyond $\xi = 1.9$ leads to a rapid increase in the size of the interior region, while the wall approaches its asymptotic shape, an antikink solution [10,11]

$$L(x) = \frac{\delta T_b}{\lambda v} \left[1 - \tanh \left(\frac{1}{\sqrt{2}\lambda} \frac{\delta T_b}{M_W} (x - X) \right) \right], \quad (17)$$

where X denotes the location of the antikink, which in the limit $\xi = 2$ moves towards infinity.

Throughout the region $1.3 < \xi < 1.8$ the thin wall approximation cannot be employed. This is also clear from Fig. 5, where we show the action densities for the temperatures $\xi = 1.3$, $\xi = 1.8$ and $\xi = 1.9$. For the potential considered, the thin wall approximation is valid only for ξ very close to 2.

In Fig. 6 we show the quantity X , defined as the position where the derivative of the Higgs field function $L'(x)$ assumes its maximal absolute value

$$X : L'(X) < 0 , \quad L''(X) = 0 . \quad (18)$$

This value of X we employ as a definition for the location of the bubble wall. It is consistent with the use of X in eq. (17) in the limit $\xi = 2$. Approaching this limit we observe a rapid increase in X . Here X can be interpreted as the bubble radius.

Fig. (6) also exhibits the quantity D

$$D = -\frac{L(0)}{L'(X)} , \quad (19)$$

which we interpret as a measure for the size of the wall. In the limit $\xi = 2$ D smoothly approaches the corresponding analytical value of the antikink

$$D = \frac{2M_H M_W}{\delta T_b v} .$$

The value of the Higgs field function at the origin, $L(0)$, is shown in Fig. 7 as a function of ξ . $L(0)$ starts from zero at $\xi = 0$, and increases with increasing ξ until about $\xi = 1.7$, where it gets close to $\langle\phi(T)\rangle$. Then it decreases along with $\langle\phi(T)\rangle$, approaching $\langle\phi(T)\rangle$ from below.

The three-dimensional action of the bubble obtained from eqs. (12) with $c = 0$ is presented as a function of ξ in Fig. 3. We find good agreement with the semi-analytic formula presented by Adams [14]. In the limit $\xi = 2$, the action diverges, and the bubble ceases to exist.

4) Normal modes

Sphalerons and bubbles are extrema of the effective action (12). None of them is a stable minimum. To exhibit their instabilities one needs to consider general fluctuations about the extremal configurations and to construct the parts of the action functional quadratic in these fluctuations. The quadratic parts then represent operator equations, whose discrete negative eigenvalues correspond to the unstable modes of the non-perturbative solutions.

By construction, the non-perturbative solutions discussed above are invariant under $SO(3)_d$, a diagonal subgroup of $SU(2)_I \times SO(3)_R$ (i. e. the group of weak isospin

and the group of spatial rotations). General fluctuations about the non-perturbative solutions can be decomposed according to the irreducible representations of $SO(3)_d$, whose contributions decouple in the quadratic form. Here, we consider only the sector of spherically symmetric fluctuations, where the instabilities of the zero-temperature sphaleron are known to reside as well as the unstable breathing mode of the bubble.

Normal modes about the sphalerons

The most general spherically symmetric fluctuations about the sphaleron consists of five radial functions

$$\Phi(\vec{x}) = \frac{v}{\sqrt{2}} \left((L(x) + \frac{\psi(x)}{\sqrt{2}x}) \mathbb{I} + i \frac{\chi(x)}{\sqrt{2}x} (\frac{\vec{x} \cdot \vec{\tau}}{x}) \right) \begin{pmatrix} 0 \\ 1 \end{pmatrix}, \quad (20)$$

$$A_i^a(\vec{x}) = \frac{M_W}{gx} \left[\left(G(x) + \psi_G(x) \right) \epsilon_{iba} \hat{x}_b + \psi_H(x) (\delta_{ia} - \hat{x}_i \hat{x}_a) + \sqrt{2} \psi_K(x) \hat{x}_i \hat{x}_a \right]. \quad (21)$$

The fluctuations ψ and ψ_G decouple in the quadratic form from the fluctuations χ , ψ_H and ψ_K [15], yielding a system of two equations (2-channel) and a system of 3 equations (3-channel), respectively,

$$\begin{aligned} \psi_G'' &= \left(L^2 + \frac{3(G-1)^2 - 1}{x^2} - \omega^2 \right) \psi_G + \frac{\sqrt{2}LG}{x} \psi, \\ \psi'' &= \frac{\sqrt{2}LG}{x} \psi_G + \left(\frac{G^2}{2x^2} + \frac{4\lambda}{g^2} \frac{d^2 V}{dL^2} - \omega^2 \right) \psi, \end{aligned} \quad (22)$$

$$\begin{aligned} \psi_K' &= -\frac{1}{x} \psi_K - \frac{\sqrt{2}(G-1)}{x} \psi_H + L\chi, \\ \psi_H'' &= \frac{2\sqrt{2}(G-1-xG')}{x^2} \psi_K + \left(L^2 + \frac{3(G-1)^2 - 1}{x^2} - \omega^2 \right) \psi_H - \frac{\sqrt{2}LG}{x} \chi, \\ \chi'' &= 2L' \psi_K - \frac{\sqrt{2}LG}{x} \psi_H + \left(\frac{(G-2)^2}{2x^2} + L^2 + \frac{4\lambda}{g^2} \frac{1}{L} \frac{dV}{dL} - \omega^2 \right) \chi. \end{aligned} \quad (23)$$

For $T = 0$, the negative mode of the sphaleron, present in the 3-channel [15], is unique for $M_H < 12M_W$ [16,17], while new directions of instability develop for $M_H \geq 12M_W$. The 2-channel possesses a single discrete positive mode for $0 \leq M_H \leq 1.5M_W$ [17].

Also for $T > 0$ the sphaleron possesses (at $M_H = 45$ GeV) a unique negative mode in the 3-channel, shown in Fig. 8. Analogous to the approximate scaling behaviour (14) of the three-dimensional action we find an approximate scaling behaviour of the eigenvalue ω^2 of the negative mode

$$\omega_{\text{sp}}^2(T) = \omega_{\text{sp}}^2(0) \frac{\langle \phi(T) \rangle^2}{\langle \phi(0) \rangle^2}, \quad (24)$$

which again is exact for an effective potential without cubic term. Using $\omega^2(0) = -1.9$, the deviation of the numerical values of $\omega^2(T)$ from the approximate scaling values (24) is on the order of 10% at $T = T_c$ (i. e. $\xi = 0$) and increases to about 20% at $T = T_b$ (i. e. $\xi = 2$).

Normal modes about the bubbles

For the discrete modes of the bubble the 2-channel eqs. (22) is the relevant channel. For the bubble the two equations of the 2-channel decouple, since $G(x) = 0$. The equation for the fluctuation ψ_G has a repulsive potential and therefore no normalizable discrete modes.

The equation for the fluctuation ψ reduces to

$$-\psi'' + \frac{4\lambda}{g^2} \left(3L^2 - \frac{6\delta T}{\lambda v} L - 1 + \frac{\gamma T^2}{\lambda v^2} \right) \psi = \omega^2 \psi . \quad (25)$$

The potential in eq. (25) is “deep enough” as to allow for a state with negative eigenvalue (i. e. $\omega^2 < 0$). This eigenmode represents the unstable breathing mode of the bubble, which lets bubbles smaller than the critical bubble shrink and larger bubbles grow. The negative eigenvalue ω^2 is presented in Fig. 9. It starts from zero at $\xi = 0$, where the bubble solution appears, and ends at zero at $\xi = 2$, where the bubble solution approaches the antikink eq. (17), which also has a zero eigenvalue. For $\xi \rightarrow 2$ the mode of the bubble indeed approaches the zero mode of the antikink

$$\psi(x) = \frac{1}{\cosh^2 \left(\frac{1}{\sqrt{2}\lambda} \frac{\delta T_b}{M_W} (x - X) \right)} , \quad \omega^2 = 0 .$$

Fig. 9 also shows approximate values for the eigenvalue ω^2 , obtained from the formula

$$\omega^2 = -\frac{2}{X^2} , \quad (26)$$

where X is defined in eq. (18). This approximate formula works amazingly well throughout the full region $0 < \xi < 2$, and not only in the vicinity of $\xi = 2$ [18], where X symbolizes the radius of the bubble.

Beside the negative mode, eq. (25) allows for a discrete positive mode, also exhibited in Fig. (9). For small values of ξ the positive eigenvalue ω^2 increases almost parallel to the continuum defined by

$$\omega^2 = \frac{4\lambda}{g^2} \left(\frac{T^2}{T_c^2} - 1 \right) .$$

When ξ approaches the limiting value of 2, however, ω^2 bends away from the continuum line. The positive mode of the bubble now approaches the positive mode of the antikink

$$\psi(x) = \frac{\sinh\left(\frac{1}{\sqrt{2\lambda}} \frac{\delta T_b}{M_W}(x - X)\right)}{\cosh^2\left(\frac{1}{\sqrt{2\lambda}} \frac{\delta T_b}{M_W}(x - X)\right)}, \quad \omega^2 = 3\left(\frac{\delta T_b v}{M_H M_W}\right)^2.$$

For the 3-channel of the bubble the equations do not decouple. Our analysis indicates, however, that there are no discrete modes in this channel.

5) Conclusion

In this paper we have studied the sphaleron and the bubble, two non-perturbative solutions of the electroweak model in the region of the electroweak phase transition. The temperature dependence of the model is taken into account via an effective potential, which assures a first order phase transition.

The sphaleron solution, its action density and in particular its three-dimensional action follow an approximate scaling behaviour with respect to the well-known zero temperature sphaleron. The action decreases with the scaling factor $\Lambda = \langle\phi(T)\rangle/\langle\phi(0)\rangle$, while the size increases with this scaling factor. At the temperature T_c the sphaleron is bigger by a factor of about 2 and at T_b it is bigger by a factor of about 3 than the zero temperature sphaleron, giving it a size of about $10 - 20M_W$ in the region of the phase transition.

The sphaleron has a single unstable mode in the region of the phase transition. The negative eigenvalue also shows an approximate scaling behaviour. Indeed, the eigenvalue ω^2 of the negative mode at finite temperature is rather well approximated by the negative eigenvalue at zero temperature scaled by the factor Λ^2 .

The bubble solution only exists for sufficiently large temperatures, $T_c < T < T_b$. In the limit $T \rightarrow T_c$ the solution converges to the trivial solution (i. e. all fields are vanishing). In the limit $T \rightarrow T_b$ the bubble solution approaches the antikink solution, where the bubble wall moves towards infinity, and the three-dimensional action diverges.

In the vicinity of the phase transition the bubble function develops an interior region where it is approximately constant, followed by the region of the bubble wall. At temperatures where the phase transition occurs, the size of both regions is of the same

order of magnitude. The thin wall approximation is not justified here. It is justified only for $T \rightarrow T_b$, where the size of the interior region rapidly increases, while the wall approaches an asymptotic shape and size, given by the shape and size of the antikink. The size of the bubble wall, being a few times the size of the sphaleron, is thus of the same order of magnitude as the size of the sphalerons at these temperatures.

The bubble has a single negative mode, the breathing mode. The frequency of this mode starts from zero at T_c and again approaches zero at T_b . For $T \rightarrow T_b$ the negative mode of the bubble and its eigenvalue approach the zero mode of the antikink. The negative eigenvalue is very well approximated by the simple formula $\omega^2 = -2/X^2$, where X is defined as the value, where the bubble function changes most strongly, i. e. $|L'(X)|$ is a maximum. For large temperatures, X may be viewed as the bubble radius.

The bubble also possesses a positive discrete mode. As a function of temperature the eigenvalue of this mode increases parallel to the continuum. However, for $T \rightarrow T_b$ the eigenvalue bends away from the continuum: the positive mode of the bubble approaches the positive mode of the antikink.

6) References

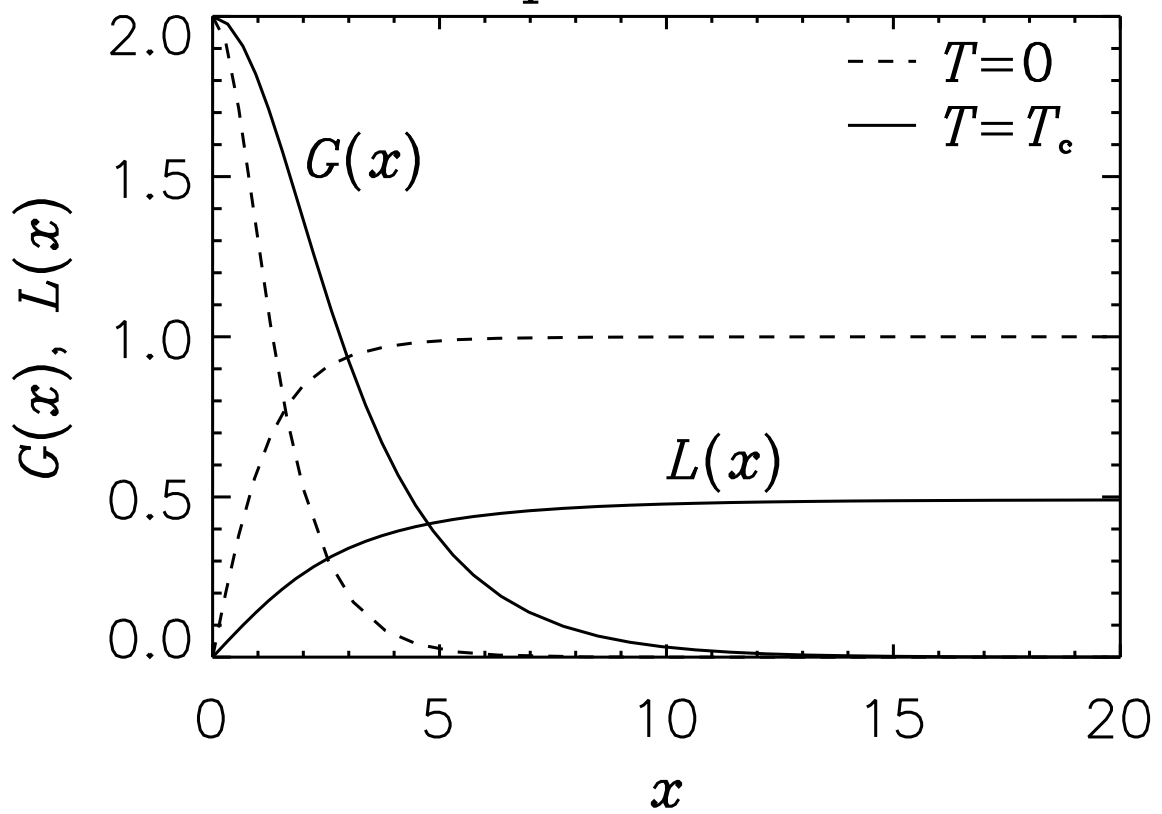
- [1] V.A. Kuzmin, V.A. Rubakov and M.E. Shaposhnikov, Phys. Lett. B155 (1985) 36.
- [2] F.R. Klinkhamer and N.S. Manton, Phys. Rev. D30 (1984) 2212.
- [3] P. Arnold and L. McLerran, Phys. Rev. D36 (1987) 581; D37 (1988) 1020.
 L. Carson and L. McLerran, Phys. Rev. D41 (1990) 647.
 L. Carson, X. Li, L. McLerran and R.-T. Wang, Phys. Rev. D42 (1990) 2127.
- [4] M.E. Shaposhnikov, Nucl. Phys. B287 (1987) 757; B299 (1988) 797; “Anomalous Fermion Number Non-Conservation” CERN-TH. 6304/91 (1991).
- [5] E.W. Kolb and M.S. Turner, “The Early Universe”, Addison-Wesley Publishing Company, Redwood City, 1990.
- [6] S. Coleman, Phys. Rev. D15 (1977) 2929.
 C. Callan and S. Coleman, Phys. Rev. D16 (1977) 1762.
- [7] A. Linde, Nucl. Phys. B216 (1983) 421.
- [8] M.E. Carrington, Phys. Rev. D45 (1992) 2933.
- [9] M. Dine, R.G. Leigh, P. Huet, A. Linde and D. Linde, Phys. Rev. D46 (1992) 550.
- [10] N. Turok, Phys. Rev. Lett. 68 (1992) 1803.
- [11] B.H. Liu, L. McLerran and N. Turok, Phys. Rev. D46 (1992) 2668.
- [12] L. Dolan and R. Jackiw, Phys. Rev. D9 (1974) 3320.
- [13] S. Braibant, Y. Brihaye and J. Kunz, “Sphalerons at Finite Temperature”, THU-93/01 (1993).
- [14] F.C. Adams, “General solutions for tunneling of scalar fields with quartic potentials”, preprint (1993).
- [15] T. Akiba, H. Kikuchi and T. Yanagida, Phys. Rev. D40 (1989) 588.
- [16] L. Yaffe, Phys. Rev. D40 (1989) 3463.

- [17] Y. Brihaye and J. Kunz, Phys. Lett. B249 (1990) 90.
- [18] D.E. Brahm, “Complex effective potentials and critical bubbles”, CALT-68-1797 (1992).

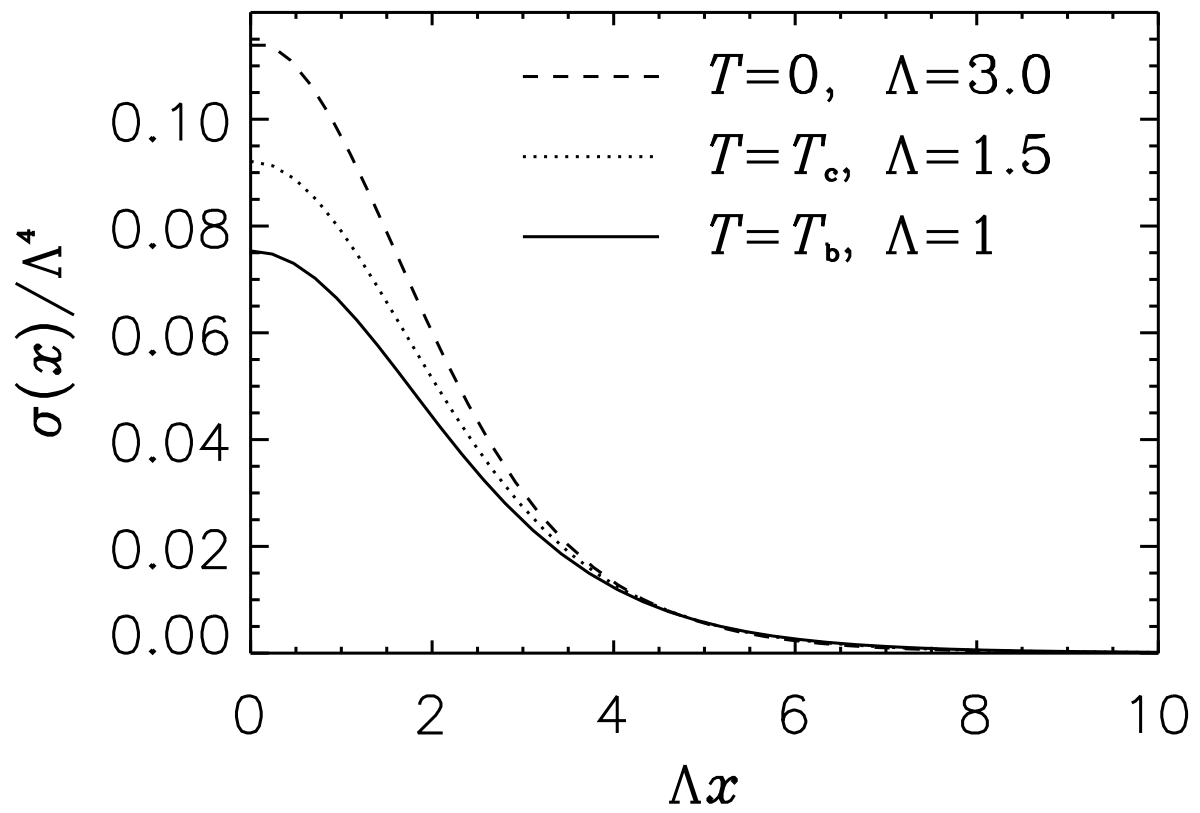
7) Figure captions

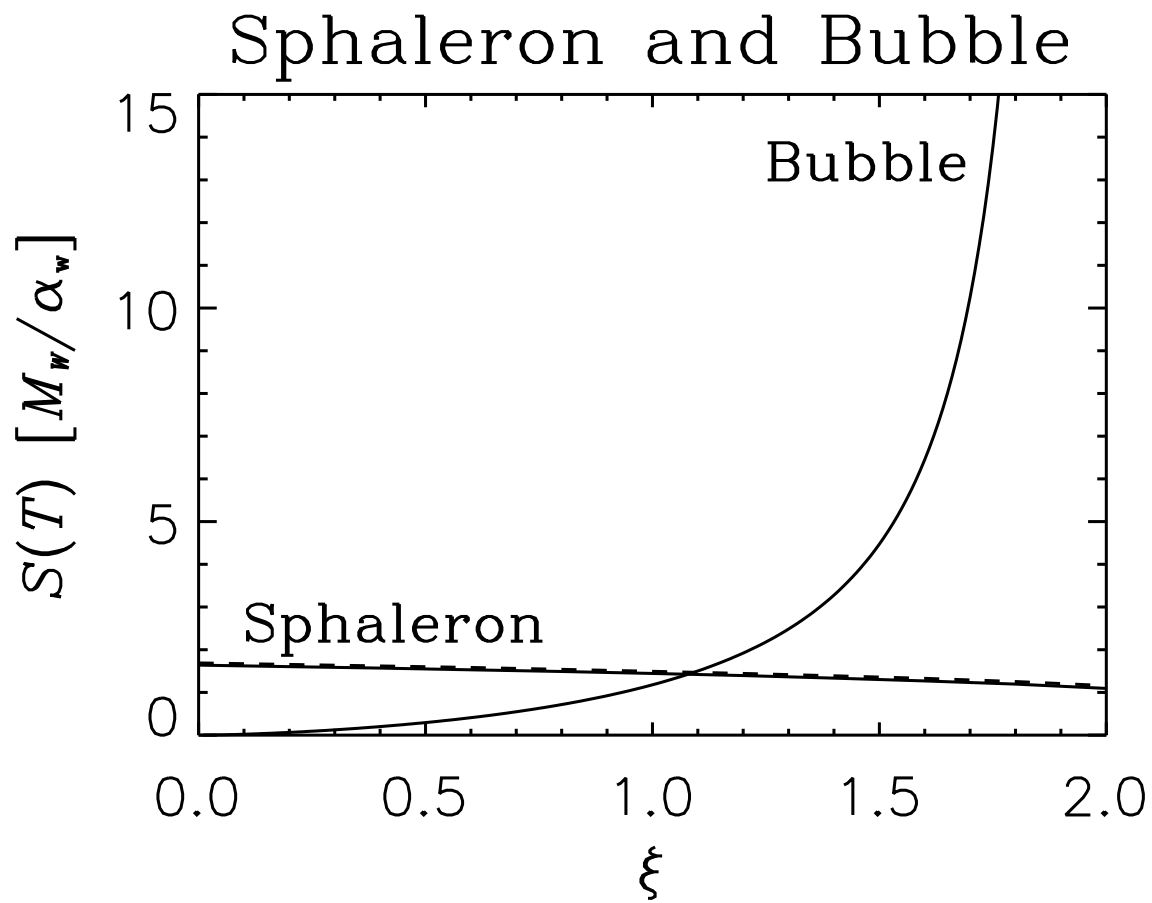
- Fig. 1 The gauge field function $G(x)$ and the Higgs field function $L(x)$ of the sphaleron are shown as a function of the dimensionless coordinate $x = M_W r$ for $T = 0$ (dashed curves) and $T = T_c$ (solid curves).
- Fig. 2 The action density $\sigma(x)$ of the sphaleron is shown as a function of the coordinate Λx for the temperatures $T = 0$ (dashed), $T = T_c$ (dotted) and $T = T_b$ (solid). Λ is the scaling factor $\langle\phi(T)\rangle/\langle\phi(T_b)\rangle$.
- Fig. 3 The action $S(T)$ of the sphaleron and of the bubble in units of M_W/α_w are shown as functions of temperature for $T_c \leq T \leq T_b$, expressed in terms of the variable ξ for $0 \leq \xi \leq 2$ (solid). For comparison the approximate scaling values for the sphaleron action are also shown (dashed).
- Fig. 4 The Higgs field function $L(x)$ is shown for the bubble as a function of the dimensionless coordinate $x = M_W r$ for the temperatures $\xi = 1.3$ (dotted), $\xi = 1.8$ (solid) and $\xi = 1.9$ (dashed).
- Fig. 5 The action density $\sigma(x)$ is shown for the bubble as a function of the dimensionless coordinate $x = M_W r$ for the temperatures $\xi = 1.3$ (dotted), $\xi = 1.8$ (solid) and $\xi = 1.9$ (dashed).
- Fig. 6 The coordinate X , where the bubble derivative $L'(x)$ has its maximal absolute value, and the quantity $D = -L(0)/L'(X)$ are shown as functions of the temperature expressed in terms of ξ .
- Fig. 7 The quantity $L(0)$ is shown for the bubble as a function of the temperature expressed in terms of ξ and compared with the minimum of the potential $\langle\phi(T)\rangle/v$.
- Fig. 8 The eigenvalue of the negative mode of the sphaleron is shown as a function of the temperature expressed in terms of ξ (solid). For comparison the approximate scaling values for the eigenvalue are also shown (dashed).
- Fig. 9 The eigenvalues of the discrete modes of the bubble are shown as functions of the temperature expressed in terms of ξ (solid). For comparison the approximate formula $\omega^2 = -2/X^2$ (dashed), and the continuum (dotted) are also shown.

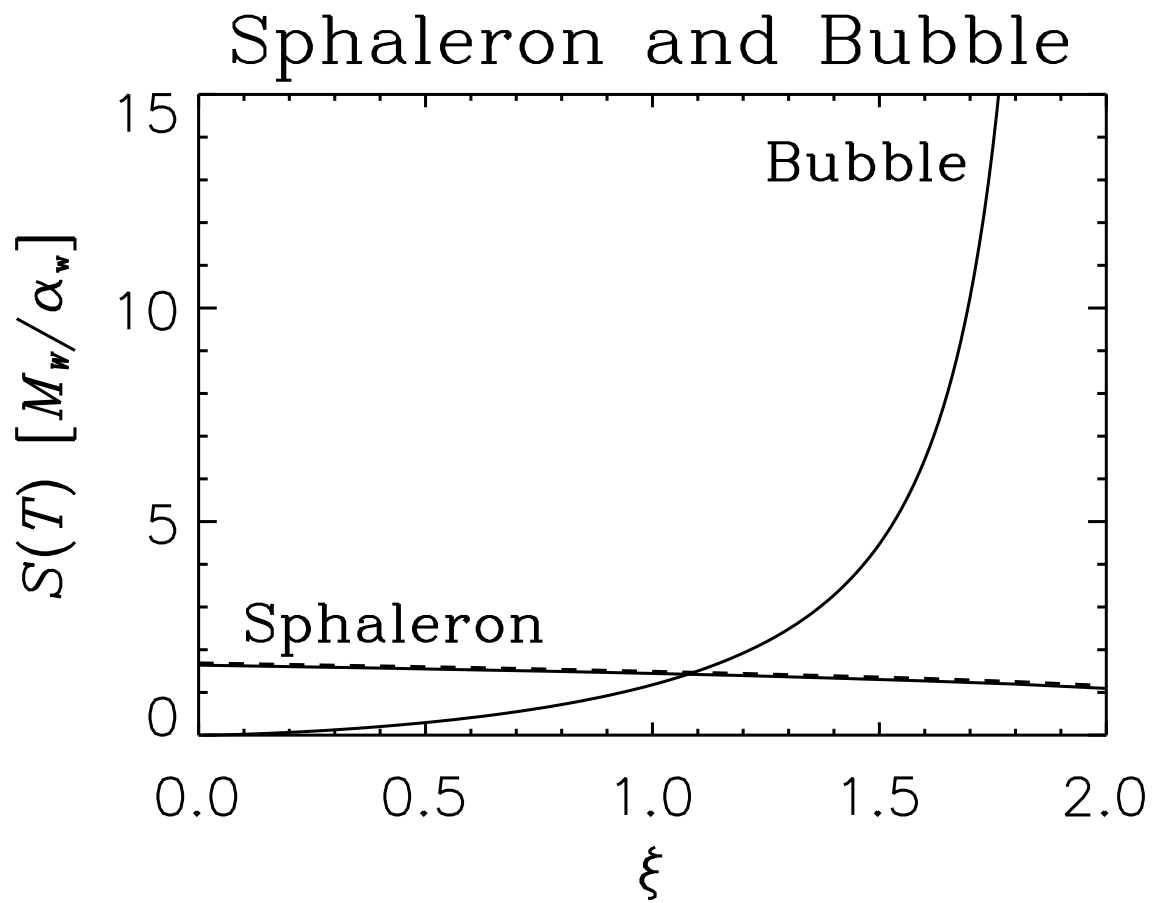
Sphaleron



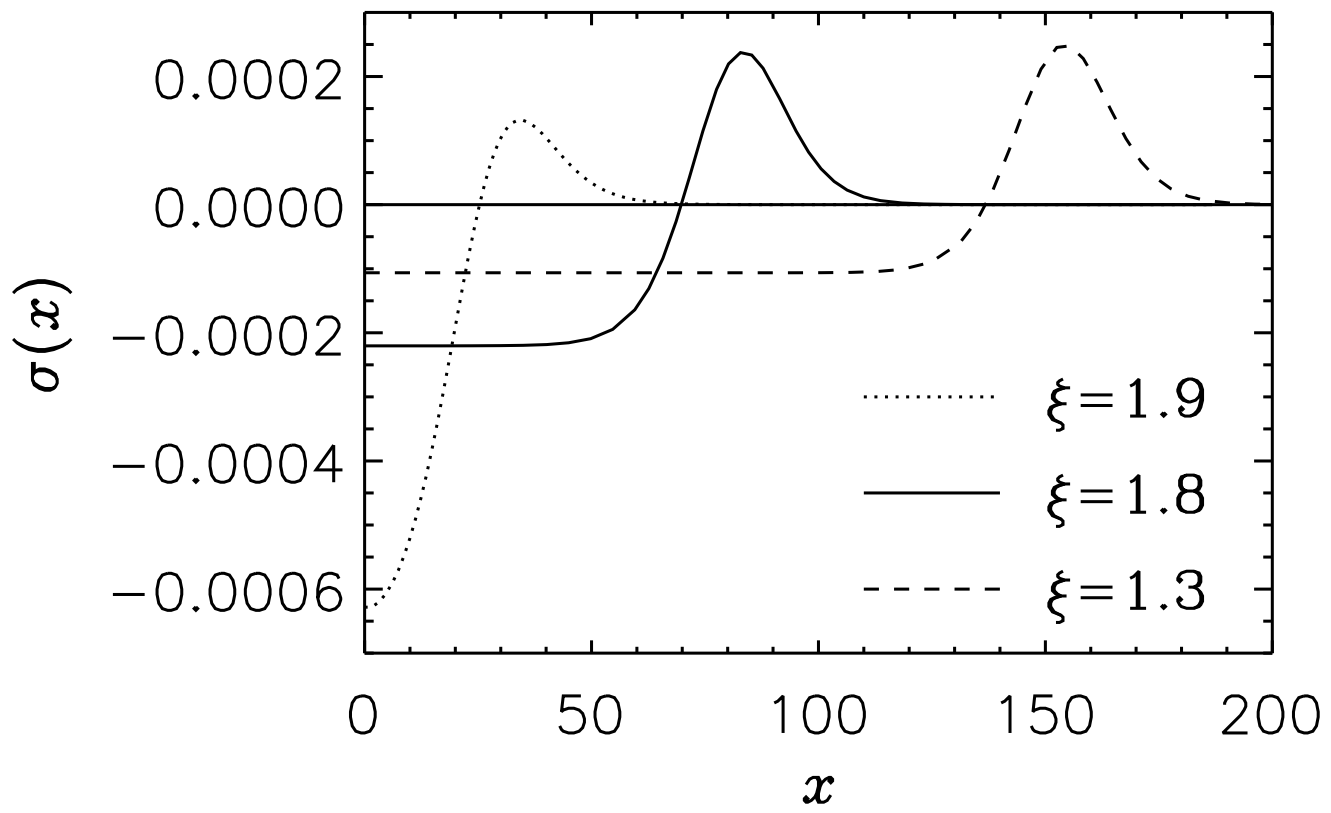
Sphaleron



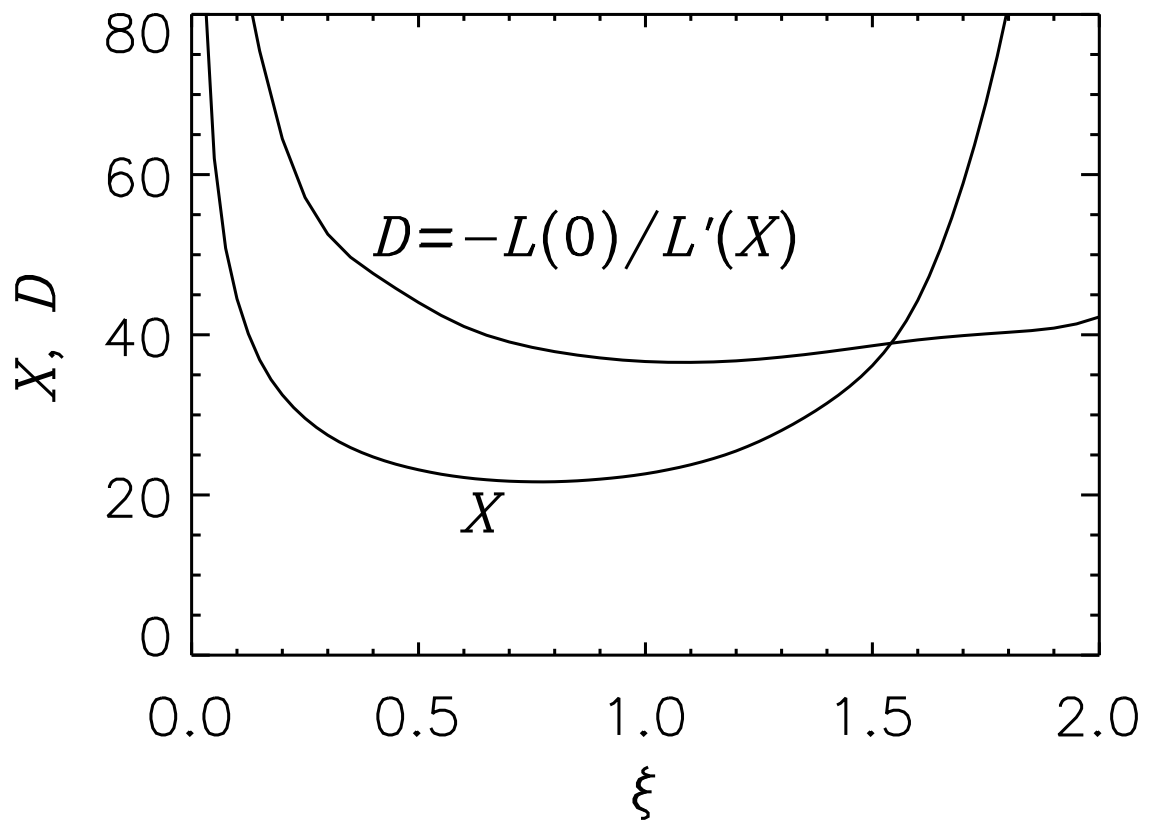




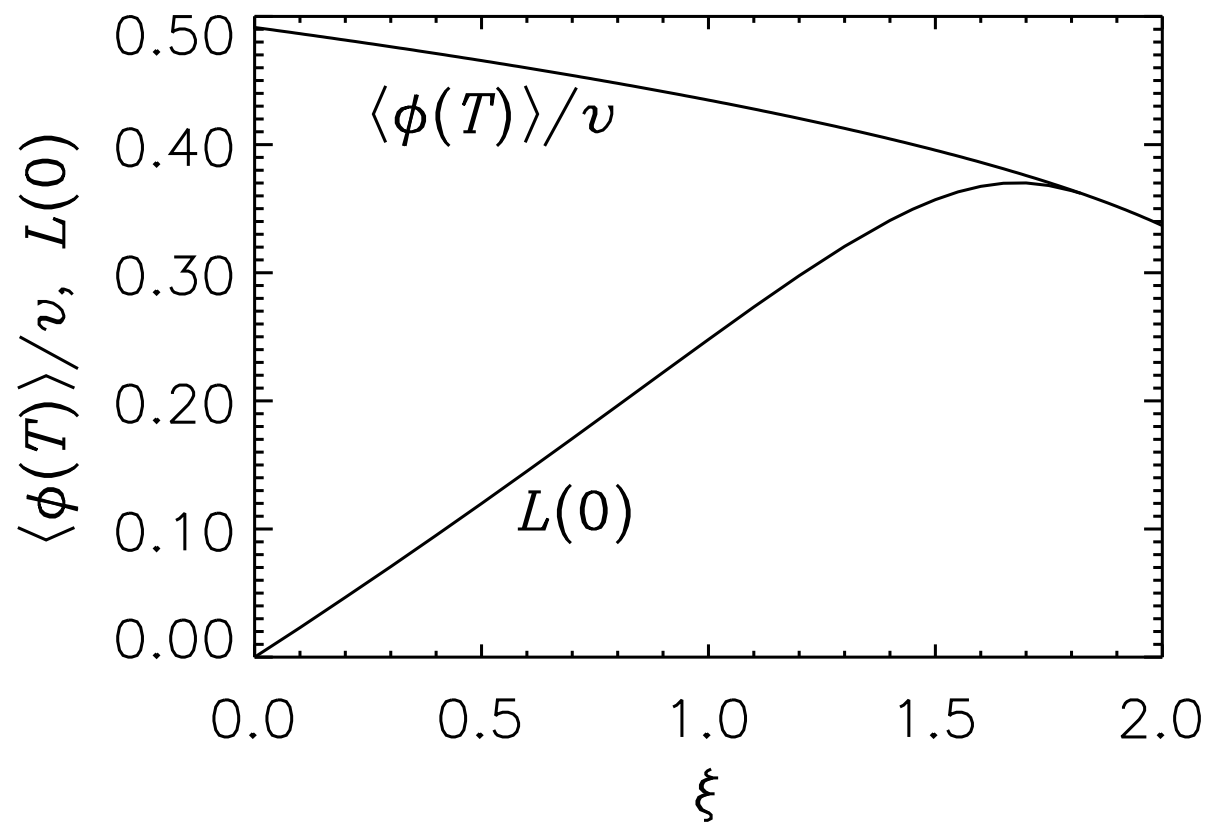
Bubble



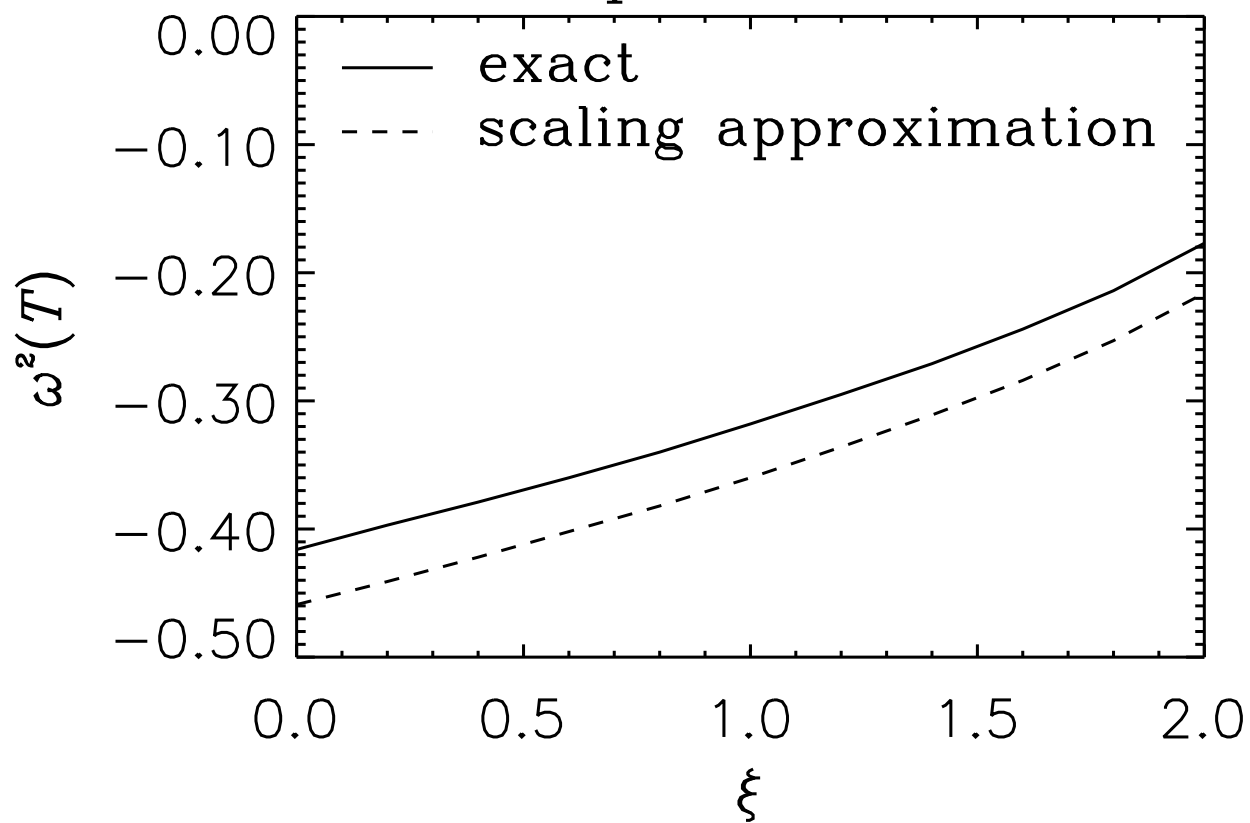
Bubble



Bubble



Sphaleron



Bubble

